ORIGINAL RESEARCH

Ferruginol potentiates the inhibition of oral cancer cell proliferation by modulating the expression of Akt-1/mTOR-mediated signaling

Pitchaimani Veerakumar, Selvaraj Jayaraman, Vishnu Priya Veeraraghavan

Abstract

Introduction: Oral squamous cell carcinoma (OSCC) is a prevalent malignancy of the oral cavity, affecting regions such as the tongue, gingiva, palate, and buccal mucosa. Ferruginol (FGL), diterpenoid derived from Podocarpus andina and Persea nubigena, has demonstrated promising biological activities, including anti-cancer potential.

Objectives: This study aimed to elucidate the molecular mechanisms underlying the anti-cancer activity of ferruginol in OSCC through integrated bioinformatics and experimental approaches, focusing on the Akt-1/mTOR signaling pathway.

Methodology: Six key target genes of FGL were identified using database analyses, and protein–protein interaction networks were constructed via STITCH and Cytoscape. KEGG enrichment analysis revealed associations with HIF-1, PI3K-Akt, and Wnt signaling pathways. In vitro experiments on KB cells evaluated oxidative stress (DCF-DA staining), morphological changes (PI and AO/EtBr staining), and antioxidant enzyme activities (SOD and CAT). Gene expression was analyzed using RT-PCR, and molecular docking was performed to assess FGL binding affinity with target proteins (NCADH, MST1, and GSK3B).

Results: Ferruginol significantly downregulated Wnt1, GSK3B, and NCADH, while upregulating MST1, VIM, and ECADH. It decreased SOD and CAT activity, increased ROS levels, and induced oxidative stress in KB cells. Docking studies confirmed strong binding affinities with key proteins involved in the Akt-1/mTOR pathway.

Conclusion: Ferruginol exerts anti-cancer effects in OSCC by modulating the Akt-1/mTOR and Wnt signaling pathways, providing valuable mechanistic insights and highlighting its potential as a therapeutic agent in OSCC management.

Keywords: Oral cancer, Ferruginol, Akt, mTOR, Phytotherapeutics, Computational methods.

Introduction

Oral squamous cell carcinoma (OSCC) is the sixth most common cancer worldwide,[1] affecting various regions of the oral cavity, including the lips, tongue, buccal mucosa, floor of the mouth, gingiva, hard palate, and retromolar trigone.[2] OSCC is characterized by rapid differentiation, proliferation, and the ability to metastasize to distant systems.[3] The survival rates for OSCC are highly dependent on the stage of diagnosis, with early detection significantly improving outcomes.[4] Potentially malignant disorders (PMDs), often presenting as clinical alterations in the oral mucosa, may precede OSCC.[5] Reactive oxygen species (ROS), byproducts of redox processes, have been strongly implicated in the development and progression of OSCC.[6] Risk factors for OSCC include tobacco and alcohol use, high-risk human papillomavirus (HPV) and Epstein-Barr virus (EBV) infections, ultraviolet (UV) radiation, and environmental pollutants.[7] In the United States alone, approximately 30,000 individuals are diagnosed with OSCC annually, with nearly 90% of oral cavity cancers attributed to this type.[8,9]

Ferruginol (FGL), a bioactive diterpenoid isolated from the stem bark of *Podocarpus andina* (Podocarpaceae) and *Persea nubigena*, has garnered attention for its diverse pharmacological properties. These include antimicrobial, antibacterial, cardioprotective,[10] antioxidant,[11] anti-plasmodial,[12] and anti-ulcerogenic activities.[13] FGL has demonstrated significant anti-cancer potential, inhibiting the proliferation of cancerous

Department and Institution Affiliation: Centre of Molecular Medicine and Diagnostics (COMManD), Department of Biochemistry, Saveetha Dental College & Hospital, Saveetha Institute of Medical & Technical Sciences (SIMATS), Saveetha University, Chennai 600077, India.

Corresponding Author: Pitchaimani Veerakumar, Centre of Molecular Medicine and Diagnostics (COMManD), Department of Biochemistry, Saveetha Dental College & Hospital, Saveetha Institute of Medical & Technical Sciences (SIMATS), Saveetha University, Chennai 600077, India. E-mail: veerakumarp.sdc@saveetha.com

How to cite the article: Veerakumar P, Jayaraman S., Veeraraghavan V P. Ferruginol potentiates theinhibition oforal cancer cell proliferation bymodulating theexpression of Akt-1/mTOR-mediated signaling. Oral Maxillofac Pathol J 2026; 17(1); 84-92.

Source of Support: Nil

Conflict of Interest: None

cells in prostate and non-small cell lung cancers.[14] Additionally, it exhibits anti-inflammatory properties by reducing the expression of inflammation-associated proteins and inducing apoptosis via NF-κB translocation and p38 phosphorylation.[15,16] Previous studies have highlighted ferruginol's effects on MCF-7 cells, suggesting its potential as a therapeutic agent for breast cancer. However, its efficacy in treating OSCC remains unexplored. This study aims to evaluate the anti-cancer effects of ferruginol on oral squamous carcinoma cells (KB cells). Further research and clinical studies are essential to comprehensively assess its safety and therapeutic potential, which could pave the way for its integration into treatment regimens for oral cancer.

Methodology

IDENTIFICATION OF POTENT DIFFERENTIALLY EXPRESSED GENES INTERACTING with FGL

The Comparative Toxicogenomics Database (CTD) and Gene Cards were used to conduct a thorough study of the dataset. These platforms were used to collect data and investigate proteins related to ferruginol, a bioactive molecule, and OSCC. The obtained data were then visually rendered using the FunRich V3.1.3 software.[17] Visualizing shared biological goals or pathways amongst the examined records, the FunRich application created a Venn diagram. This intersection proved extremely helpful in understanding the complex molecular landscape of oral cancer.

BUILDING A PHYSIOLOGICAL PATHWAY USING THE STRING DATABASE FOR FGL

The STITCH network has been utilized to investigate the Drug-Protein Interactions (DPI) structure after it was built using differentially expressed genes (DEGs) from OSCC databases.[18] The network was shown using Cytoscape software, where edge widths dependent on interaction intensity were utilized to represent protein-protein interactions (PPI).[19] This picture was improved even further by the cytohubba plugin, which showed gene clusters that probably correspond to functional units or pathways. This investigation sheds light on possible molecular pathways and interactions related to oral cancer.

GENE ONTOLOGY AND ENRICHED PATHWAY ANALYSIS FOR FGL

Using genome data, a thorough functional and pathway enrichment study of DEGs in oral cancer was carried out. The study found enriched KEGG pathways linked to DEGs and categorized genes into molecular functions, cellular components, and biological processes. This method offered comprehensive insights into the pathways and functional roles of genes that are up-regulated in oral cancer.

MOLECULAR DOCKING

The study examines how ferruginol binds to proteins such as VIM, ECADH, NCADH, Wnt1, MST1, and GSK3B using protein structures from the Protein Data Bank. PyRx software was used for docking using the 100-cycle Lamarckian

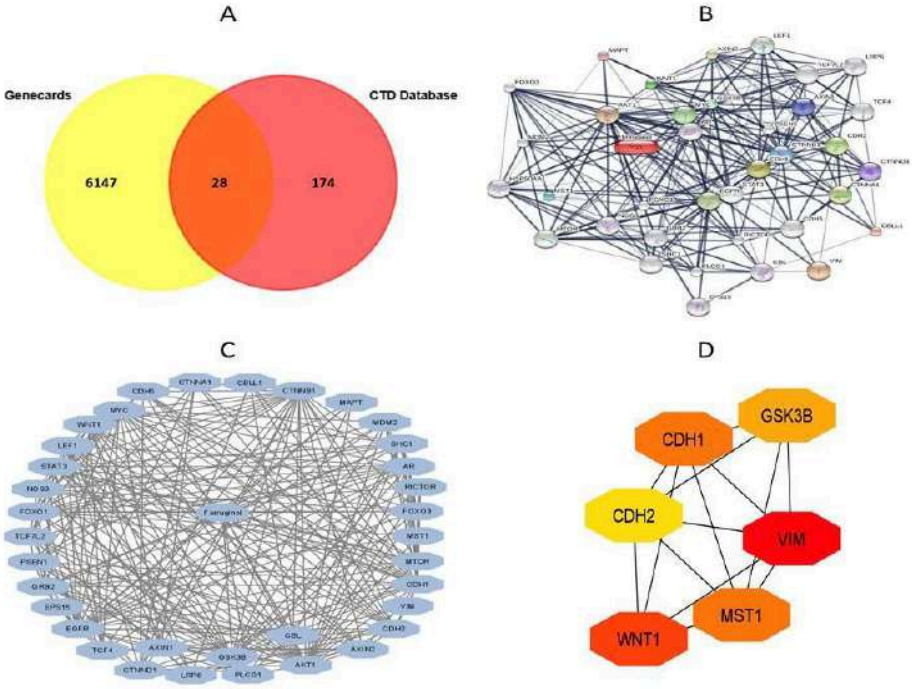

Fig. 1: Shows how the pharmacological network analysis of ferruginol corresponds to potent OSCC targets. (A) The OSCC regulating targets from Genecards and the frequently overlapping important targets for ferruginol regulation from the CTD database overlap, as shown in a Venn diagram created with the use of the Funrich tool. (B) The relationship between the material and its strongly associated principal targets was demonstrated using STITCH, a networking tool for drug-protein interactions. (C) The application Cytoscape is used to illustrate the interactions between proteins. (D) The Cytohubba plugin for the Cytoscape program additionally displays the top six significant targets.

genetic algorithm (LGA). Using Discovery Studio, the 3D and 2D structures were examined, providing insight into the interactions between ferruginol and these significant proteins. 20

CELL LINES

These KB cell lines were cultivated in a CO2 incubator at 37°C in a regulated, humidified atmosphere. The cells were kept in Dulbecco's Modified Eagle's Medium (DMEM) with 10% fetal bovine serum (FBS) and 1% penicillin-streptomycin antibiotics to promote cell growth.

CELL VIABILITY ASSAYS

The KB cell line was subjected to both MTT and trypan blue exclusion tests to evaluate the cytotoxicity of FGL.[21] After seeding and incubating for the entire night, a 1×10^4 cell population was created. Following a period of time, the cell culture was exposed to the MTT substance, which was then dissolved in DMSO. The result was determined by measuring the absorbance at 590 nm.

METABOLIC ASSAYS

Placed into 96-well plates, 1×10^4 KB cells were cultured for a whole day.[22] After being cultured for a further twenty-four hours, the cells were subjected to a second round of ferruginol treatment, and twice they were washed using Krebs-Ringer-phosphate-HEPES (KRPH) buffer. As directed by the manufacturer, glucose uptake was assessed using a colorimetric kit. The cells were removed after pre-treatment, and a colorimetric kit was used to quantify the amount of lactate levels, and deproteinized with 5% trichloroacetic acid (TCA). After treating KB cells with ferruginol, the lactate enzymatic mix was added, and the optical density (OD) was monitored at 450 nm to assess lactate enzyme activity.

MEASUREMENT OF CELLULAR SOD ACTIVITY

FGLwas applied to KB cells for 48 hours at a dose of 1×10^6 cells. WST and the enzyme functioning solution were added to 96-well microtiter plates, which had been quantified using the Bradford test for total protein, in order to evaluate the activity of the superoxide dismutase enzyme by SOD Assay Kit-WST from Fluka Co. After the plates were incubated for 10 mins at 25°C to produce a water-soluble formazan dye, absorbance was measured at 450 nm using a microplate reader.

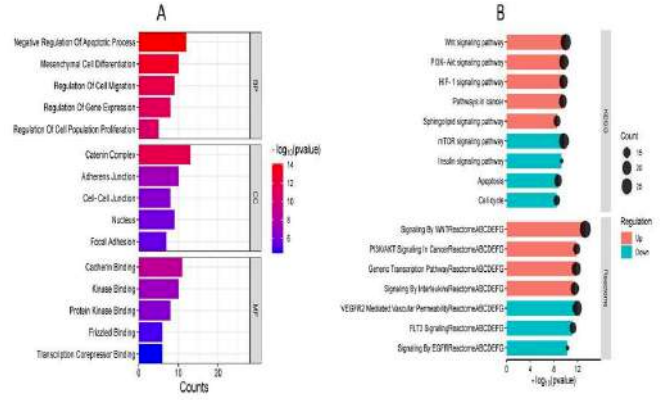

Fig. 2: Shows the gene ontologies and enriched routes for key targets in the OSCC dataset. (A) Gene ontologies for the functions of molecules, chemical reactions, and cellular parts were shown using a bubble chart. (B) Genes were classified into metabolic activities, organismal systems, cellular processes, processing of environmental information, and disorders of humans; the KEGG pathway was assigned a high enrichment score.

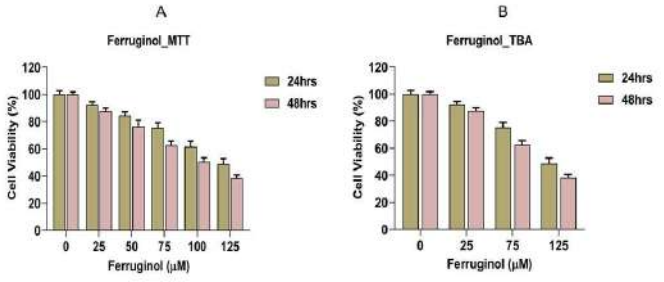

Fig. 3: Ferruginol (A and B) inhibits the growth of KB cells.

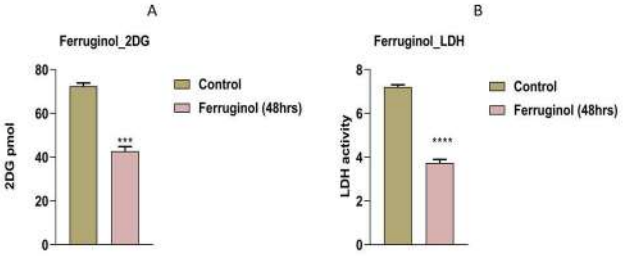

Fig. 4: In KB cells, ferruginol promotes aerobic glycolysis. (A and B). After being exposed to ferruginol for 48 hours, the amount of lactose produced and glucose absorbed by KB cells was assessed.

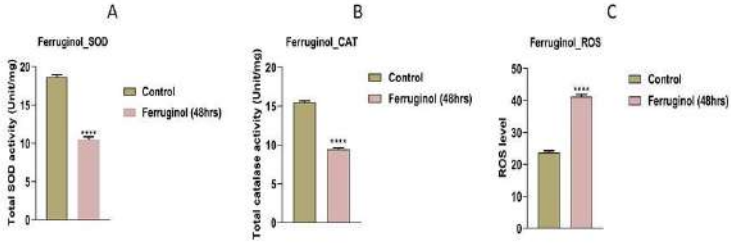

Fig. 5: In KB cells, ferruginol demonstrates antioxidant properties. (A, B, and C). Using a significance level, KB cells were treated with ferruginol to measure intracellular ROS, cellular SOD, and CAT using DCF-DA.

MEASUREMENT OF CELLULAR CATALASE ACTIVITY

The rate of action of the intracellular catalase enzyme was measured using a catalase test kit from Sigma-Aldrich. For a full day, KB cells were exposed to 1 × 10^6 cells of FGL. The cells were treated, then lysed, and the lysates were collected and washed in PBS. The samples were put into a microcentrifuge tube together with the assay buffer (50 mM KH_2PO_4/50 mM Na_2 HPO_4, pH 7.0). After adding a 200 mM H_2O_2 solution, the reaction was allowed to begin and was then incubated at 25°C for five minutes. After adding a stop solution, the mixture was incubated for 10 minutes at 25°C to produce a red quinonimine hue. At 520 nm, the absorbance was then determined.

DCFH-DA MEASUREMENT OF INTRACELLULAR ROS ACTIVITY

Intracellular ROS generation was measured using the fluorescent dye probe DCFH-DA.

In short, 1×104 KB cells were pre-treated with FGL in a time-dependent manner after being seeded the day before. Following a PBS wash, cells were treated with 10 µM DCFH-DA for 15 minutes at 37°C in the dark. Following extraction, each specimen was incubated with the lactate enzymatic combination for one hour. The OD value was then calculated by measuring the gathered specimens at 525 nm.

DCFH-DA AND PI-BASED IMMUNOFLUORESCENCE STAINING

Immunofluorescence labeling was used to visualize the morphological alterations that ferruginol treatment caused in KB cells. The production of ROS within cells was assessed using a 5-µM concentration of the non-fluorescent intracellular probe 2′,7′-dichlorofluorescein-diacetate. FGL was applied to 5×105 KB cells in the experimental setting for 40 minutes. Following the addition of DCFH-DA, the cells were cultivated for a further 20 minutes at 37 °C without light. Cells were resuspended in 1.0 mL of ice-cold phosphate-buffered saline (PBS) after this incubation period. Using a Zenoptik camera and an Olympus fluorescent microscope (Tokyo, Japan), the oxidative activity of ROS on DCFH was observed.

AO/ETBR NUCLEAR STAINING

To identify apoptotic cells for nuclear labeling with AO/EtBr staining, this was done. This staining technique uses ethidium bromide (EtBr) and acridine orange (AO) to differentiate between apoptotic and normal cells. During the experiment, a coverslip was used to evenly distribute 10µL of AO/EtBr solution over the KB cells that had received ferruginol treatment. Apoptotic cells were identified by their characteristic red fluorescence, which was brought on by fragmented nuclei and compacted chromatin when viewed under an upright fluorescent microscope. The existence of normal cells, on the other hand, was measured using Image J software and examined using an Olympus fluorescent microscope (20x magnification) in the presence of green fluorescence.

GENE EXPRESSION BY RT-PCR

KB cells were cultivated overnight after being planted in a 6-well plate at a density of 5×10^6 cells per well. Using TRIR from Abgene, UK, RNA was separated, and its amount was measured spectrophotometrically in micrograms (µg). In

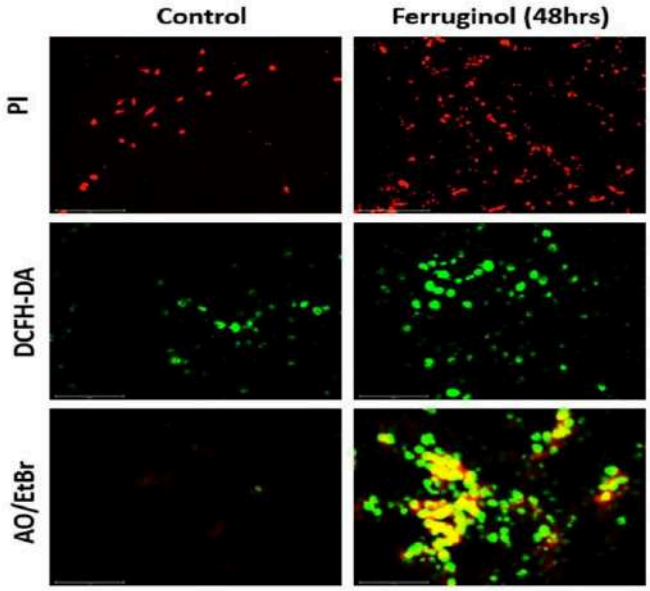

Fig. 6: Ferruginol's effects on apoptosis and ROS activity in KB cells. KB cells were exposed to ferruginol for 24 and 48 hours, and immunofluorescence labeling was used to identify any morphological alterations. AO/EtBr labeling for early and late apoptosis in KB cells, DCFH-DA for intracellular ROS activity, and PI for nuclei staining at a 20X magnification. ImageJ was used to quantify the images, and Olympus used a Zenoptik camera to display them.

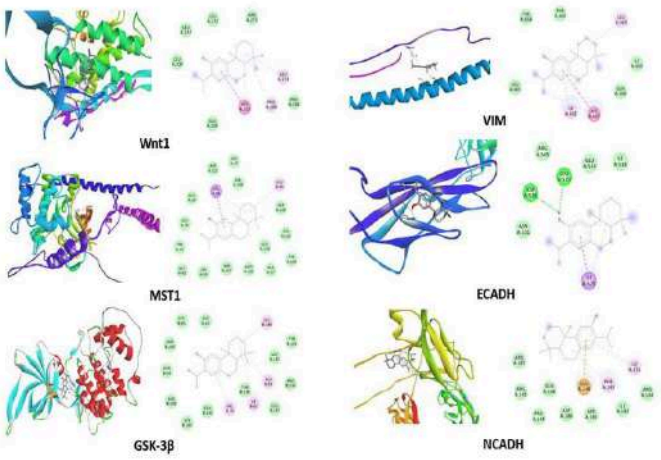

Fig. 7: Molecular docking illustrates the relationship between ferruginol and important OSCC targets. The binding affinity of ferruginol for targets is demonstrated using a molecular docking investigation performed with PyRx software. Utilizing Biovia Discover Studio, it was possible to see the 3D and 3D structural representations that have been tackled above.

order to investigate mRNA expression using real-time PCR, a reaction combination was carefully created using Takara SyBr green master mix and specially made forward and reverse primers that target specific genes, such as Wnt1, MST1, GSK3B, VIM, ECADH, and NCADH. The fold change in relation to the control was used to express the analysis's findings.

STATISTICAL ANALYSIS

The study was conducted using R, a robust statistical programming system, and the log-rank test and *p-values* for mRNA and protein expressions were computed using GraphPad Prism 8.

Results

PHARMACOLOGICAL NETWORKING METHOD OF FGL

Genomics resources like Genecards and the Comparative Toxicogenomics Database (CTD) can be searched to find genes associated with FGL and its potential effects on oral squamous cell cancer (OSCC). A Venn diagram (Graph 1A) was made to show the shared targets that were found by examining these databases and were linked to both FGL and OSCC. Approximately 28 genes were discovered to be consistently frequent across all datasets after these resources were combined. This implies that the OSCC associated with FGL may be significantly influenced by these genes. The study used the STITCH database to undertake network analysis in order to validate the 28 discovered targets related to FGL. By utilizing the STITCH database, the findings displayed in Graph 1B clarified the regulatory connections between ferruginol and targets. Then, using Cytoscape, a network was constructed (Graph 1C). To conduct a more thorough analysis, the CytoHubba plugin was employed. Wnt1, MST1, GSK3B, VIM, ECADH, and NCADH are the top six important targets with high scores, according to the results displayed in (Graph 1D). These specific targets have been thoroughly investigated due to their importance in the development of oral cancer. This comprehensive approach provides relevant information about the targets' potential significance in OSCC and boosts confidence in the identification of targets connected to FGL.

FUNCTIONAL ANNOTATIONS LINKED TO FGL IN OSCC

Once ferruginol targets have been thoroughly examined, Gene Ontology (GO) and pathway enrichment studies are necessary to comprehend the functional importance of genes associated with OSCC. For biological processes (BP), cellular components (CC), and molecular functions (MF), a bubble

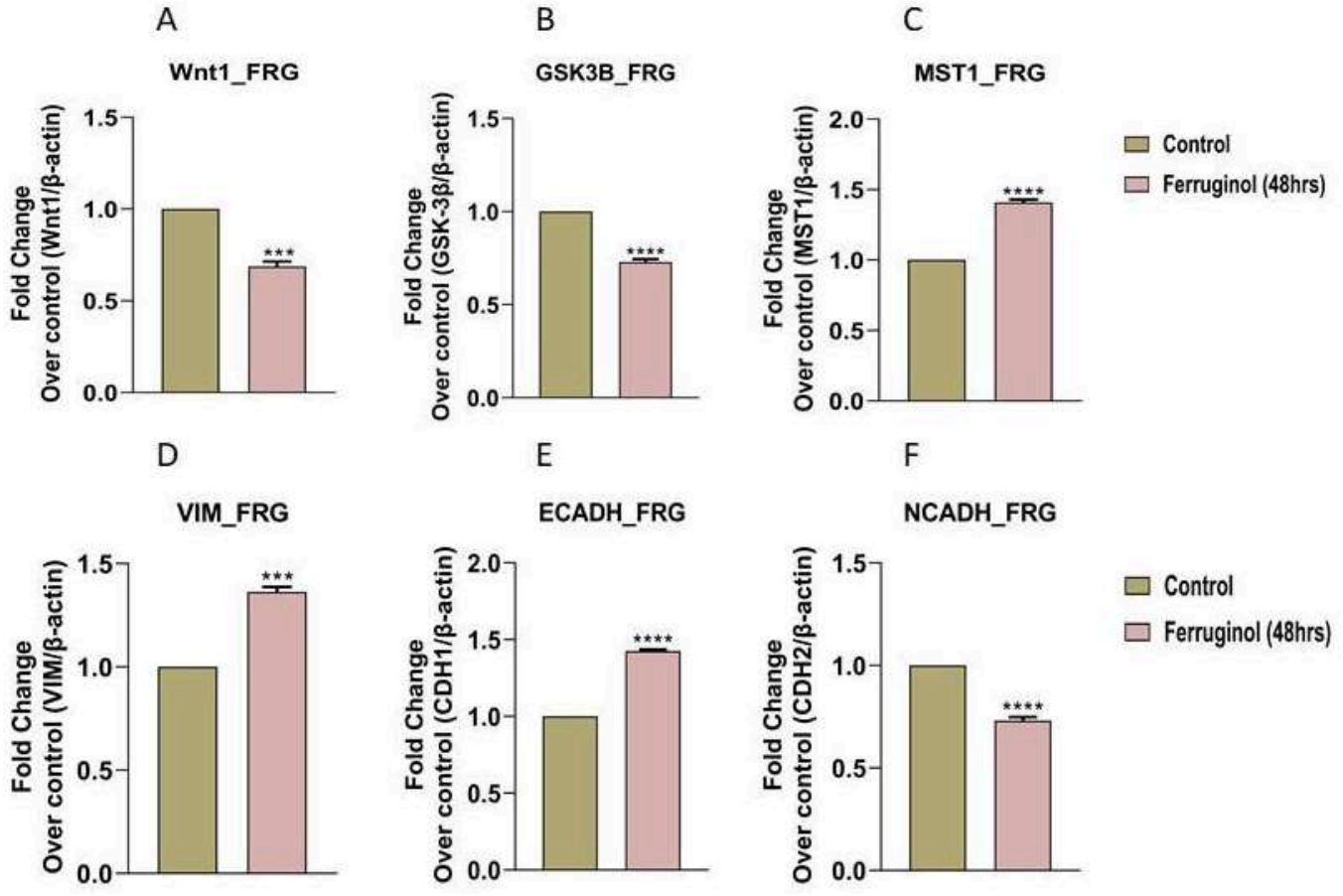

Fig. 8: Ferruginol inhibits the expression of important AKT1/mTOR signaling targets (A–F) in KB cells. Using RT-PCR, the effects of ferruginol-potent primary targets (Wnt1, VIM, GSK3B, MST1, ECADH, and NCADH) on gene expression were evaluated in KB cells.

graphic (Graph 2A) was made using g datasets to display the top five highly enriched GO terms. Research has revealed that these targets govern vital biological functions, including but not limited to cell division, apoptosis, and the regulation of gene expression. The nuclear membrane, bounded organelle, and intracellular membrane were associated with these targets. Cadherin binding, kinase binding, and protein-kinase binding were a few of their molecular actions. Extra details were revealed by KEGG pathway analysis, which showed a substantial enrichment in pathways related to cancer, PI3K-Akt pathways, HF-1 signaling, and Wnt signaling. Several genes of interest were shown to be prominent in networks relevant to malignancies, as shown in Graph 2B. Its all-encompassing method clarifies the complex web of dysregulated pathways in oral cancer and advances our knowledge of the functional significance of FGL.

FGL SUPPRESSES BOTH AEROBIC GLYCOLYSIS AND CELL GROWTH IN KB CELLS

The combined synergy between computer analysis and experimental research, including cell line investigations, increases the likelihood of discovering safe and effective therapeutic drugs. This expedites the process of developing new drugs. The cytotoxic effects of ferruginol on KB cells in the setting of oral cancer were thoroughly assessed using the MTT and trypan blue tests. For 24 and 48 hours, KB cells were treated with varying concentrations of FGL (20–100 μM). The results, which are displayed in Graph 3A, demonstrate that the gradual infusion of ferruginol into KB cells led to a significant and dose-dependent decline in cell viability. The results were further supported by the trypan blue assay (Graph 3B), which demonstrated that ferruginol treatment for 24 and 48 hours prevented KB cells from proliferating. Further evidence that lactose production and glucose absorption are hindered in KB cells is provided by the time-dependent injection of FGL in Figures 4A and B. Together, our results show that FGL inhibits aerobic glycolysis and kills oral cancer cells.

FGL ON ANTI-OXIDANT ACTIVITY IN KB CELLS

The levels of the enzymes catalase (CAT) and superoxide dismutase (SOD) have declined, according to the results displayed in Graph 5(A and B). This suggests that FGL influences ROS activity in oral cancer cells. This experimental method sheds more insight into how FGL influences ROS activity and emphasizes the molecule's possible significance in treating oral cancer. Following FGL injection, DCF-DA staining revealed increased ROS activity (Graph 5C), highlighting the importance of ROS regulation in the growth of cancer cells. The assessment of CAT and SOD activities provides further evidence that ferruginol controls ROS in KB cells.

KB CELL MORPHOLOGICAL CHANGES AS A RESULT OF FGL TREATMENT

We administered the IC50 concentrations of ferruginol to KB cells for 24 and 48 hours while monitoring for any cytomorphological changes in order to verify the drug's efficacy. The results demonstrated that the size and characteristics of the untreated cells remained unchanged. In contrast, significant cytomorphological changes, including cell shrinkage, blebbing, and cases of cell death, were observed when the treated cells were tagged with PI and DCFH-DA. To corroborate these results, we investigated ROS activity in KB cells treated with FGL. The findings demonstrated that when DCFH-DA dye is added, untreated KB cells exhibit reduced ROS activity. Additionally, KB cells' apoptotic rate was assessed by AO/EtBr nuclear staining. Interestingly, FGL treatment to KB cells over a 24- and 48-hour period caused both early and late apoptosis, as Graph 6 demonstrates. Remarkably, at 48 hours, a significant percentage of cells in the FGL-treated group were seen to be undergoing both early and late apoptotic processes. The potential therapeutic efficacy of FGL in the treatment of oral cancer is increased by these investigations, which offer

Compound	Protein(s)	Binding energy (Kcal/mol)	No. of amino acid residues	Amino acid residues
Ferruginol (CID: 442027)	Wnt1	-6.8	1	GLU204
	MST1	-8.3	1	GLY108
	GSK3B	-7.9	2	THR138, GLN185
	VIM	-6.0	1	HIS437
	ECADH	-6.9	2	ASP528, LEU533
	NCADH	-8.1	1	ASN249

Table 1: The molecular docking data for FGL with Wnt1, MST1, GSK3B, VIM, ECADH, and NCADH.

significant insights into the mechanisms of oxidative stress, apoptosis, and cellular responses associated with the treatment.

FGL SHOWS HIGH BINDING ASSOCIATION WITH AKT1/MTOR SIGNALING TARGETS

The binding energies provide significant data about the effectiveness of these interactions, as illustrated in Graph 7 and summarized in Table 1. Apoptosis, metabolism, and cell growth are all affected by these proteins. The binding energies of ferruginol were significantly high when it interacted with several important proteins, such as Wnt1 (-6.8 Kcal/mol), MST1, GSK3B, VIM, ECADH, and NCADH. These targets were also found to bind to a significant number of hydrogen-bonded amino acid residues, including those associated with Wnt1 (GLU204), MST1 (GLY108), GSK3B (THR138, GLN185), VIM (HIS437), ECADH (ASP528, LEU533), and NCADH (ASN249).

KB CELLS, FGL PROMOTES AKT1/MTOR SIGNALLING TARGETS

The study also employed real-time PCR to assess the mRNA expression levels of many genes essential for aerobic glycolysis and apoptosis when KB cells were exposed to FGL at IC50 values for 24 and 48 hours. First, as shown in Graph 8(C, D, and E), FGL treatment resulted in a significant rise in the mRNA expression of the apoptotic genes, which regulate targets MST1, VIM, and ECADH. In an average of 24-48 h, this growth happened. Graph 8 (A, B, and F) illustrates the genes that belong to this group: they are involved in the suppression of apoptosis, aerobic glycolysis, cell division, and protein synthesis. NCADH, Wnt1, and GSK3B were among these genes. The findings indicate that the administration of FGL in KB cells could potentially affect the AKT1/mTOR signaling pathway, in addition to other possible consequences.

Discussion

Oral squamous cell carcinoma (OSCC), the most prevalent form of oral cancer,[24] is characterized by aggressive tumor growth, early metastasis, and poor survival rates, with a 5-year survival rate of less than 50%.[25,26] Risk factors such as tobacco use, alcohol consumption, and betel nut chewing are particularly significant in regions like Taiwan.[27] These behaviors contribute to the accumulation of ROS, which play a key role in the progression of OSCC. The pressing need for effective therapeutic agents against OSCC has led to investigations into bioactive compounds such as FGL, an abietane diterpene with broad pharmacological properties, including anti-cancer potential.

One of the main forms of oral cancer is called OSCC, and it can be linked to a number of carcinogens from oral behaviors like drinking alcohol, smoking cigarettes, and chewing betel quid.[28] Head and neck carcinoma, the sixth most frequent cancer worldwide, primarily has OSCC as its histological type.[29,30] By reducing MMP, increasing ROS, lipid peroxidation, decreasing cell viability, and increasing antioxidant enzymes, FGL can exert an anti-cancer effect in HCT-116 cells. Thus, while Bcl-2 is being suppressed, FGL induces apoptosis via a mitochondrial-mediated route, improving the expression of caspase-3, cytochrome c, Bax, and caspase-9 in HCT-116 cells. The reason behind FGL's induction of mitochondria-regulated apoptosis in human colon cancer cells is still unknown. The goal of the current study was to reveal the FGL's mitochondrial-mediated apoptotic cascade in HCT-116 cells.[31] In human ovarian cancer cells (OVCAR-3), FGL may have anti-cancer effects by causing G2/M cell cycle arrest, death, and inhibition of cancer cell migration. When considered collectively, FGL may be helpful in ovarian cancer.[32] SK-MEL-28 cells, FGL converted to 18-aminoferruginol boosts its antiproliferative activity five times and modifies the apoptotic pathway to activate caspases 3/7 without first depolarizing the mitochondrial membrane. 18-aminoferruginol is more cytotoxic to a panel of 60 cancer cells than its parent molecule, which is consistent with in silico expectations.[33] By inducing mitochondrial apoptosis, FGL suppresses the development of thyroid cancer cells. Additionally, it produced ROS, lowered MMP levels, and blocked the PI3K/AKT and MAPK signaling pathways. FGL considerably reduced the disease activity index and spleen weight while increasing body weight, colon weight, and colon length.[34] Our study showed the potential of FGL as a treatment for OSCC was investigated through a multidisciplinary approach that included route enrichment studies, database mining, and network analysis. Initial identification of genes linked to FGL and OSCC regulatory targets was performed using databases like Genecards and the Comparative Toxicogenomics Database (CTD). The combined datasets revealed 28 overlapping genes, suggesting that these genes could be significant targets for FGL in OSCC. Network analysis showed important regulatory connections between FGL and its targets, with key genes such as Wnt1, MST1, GSK3B, VIM, ECADH, and NCADH emerging as critical in the development of oral cancer. This analysis reinforced the relevance of these targets in OSCC pathophysiology, providing valuable insights into their roles. GO and pathway enrichment analyses further supported these findings, highlighting the significance of these targets in processes like apoptosis, cell differentiation, gene regulation, and cell migration. KEGG pathway analysis also revealed significant enrichment in pathways related to cancer, PI3K-Akt signaling, HIF-1 signaling, and Wnt signaling, all of which are implicated in OSCC. FGL's potential role in restoring these dysregulated pathways suggests its therapeutic promise in oral cancer treatment.

To evaluate the cytotoxic effects of FGL on OSCC, we employed both computational and experimental approaches. The impact of different FGL dosages on KB cells was assessed using MTT and trypan blue assays over 24 and 48 h. These assays revealed a significant, dose-dependent decrease in cell viability, with the half-maximal inhibitory concentration (IC50) identified after treatment. These findings were corroborated by the trypan blue test, which demonstrated that FGL inhibited KB cell proliferation. Furthermore, FGL treatment led to slower lactate generation and glucose absorption in the cells, indicating interference with aerobic glycolysis, a vital process in cancer development. The role of FGL in regulating reactive oxygen species (ROS) activity was also examined using catalase (CAT) and superoxide dismutase (SOD) activity assays. FGL treatment reduced CAT and SOD activity, suggesting that it regulated ROS levels in KB cells. DCF-DA staining confirmed

increased ROS production in treated cells, highlighting FGL's involvement in ROS modulation in cancer cells. These results underline the potential of FGL to target ROS-mediated pathways in oral cancer treatment. Notable morphological changes, including cell shrinkage, blebbing, and instances of cell death, were observed in KB cells treated with FGL at IC50 concentrations for 24 and 48 h. Cytomorphological analysis using PI and DCFH-DA staining confirmed the onset of both early and late apoptosis, as indicated by nuclear staining with AO/EtBr. These observations provide strong evidence of FGL's therapeutic efficacy in inducing apoptosis in oral cancer cells.

Real-time PCR analysis revealed significant changes in the expression of genes associated with apoptosis and aerobic glycolysis following FGL treatment. The mRNA expression of apoptotic genes MST1, VIM, and ECADH increased significantly, while genes involved in protein synthesis, cell division, and glycolysis, such as Wnt1, GSK3B, and NCADH, showed altered expression levels. These findings suggest that FGL modulates the AKT1/mTOR pathway, which is crucial for cancer cell proliferation. Molecular docking simulations revealed that ferruginol (FGL) binds strongly to key cancer-related proteins such as Wnt1, GSK3B, NCADH, MST1, VIM, and ECADH, enhancing our understanding of its anti-cancer effects. FGL targets multiple pathways involved in cell growth, metabolism, and apoptosis, making it a promising oral cancer treatment. Further research is needed to optimize its formulation and distribution for clinical use. Despite current limitations, FGL shows significant therapeutic potential for OSCC. Future studies should focus on maximizing its efficacy and clinical application.

Conclusion

FGL exhibited significant therapeutic potential against OSCC by targeting key molecular pathways. Combining laboratory testing with computational biology, it binds securely to key proteins. FGL caused apoptosis in cells, impacted metabolic regulation, and raised oxidative stress by modifying the Akt-1/mTOR signaling pathway. According to our research, FGL may be used to treat oral cancer. Both analytical and laboratory data back this conclusion. The research may take new turns in the future by combining treatments to maximize benefits and reduce side effects. This could lead to the creation of novel treatment plans for OSCC. Targeted therapy that utilizes FGL's effects on the mTOR pathway may also progress customized cancer treatment. To fully exploit FGL's therapeutic potential and enhance patient outcomes, more research is required into the clinical translation of this drug, its interactions with other signaling pathways, and its broader utility in cancer treatment.

References

1. Lee KC, Chuang SK, Philipone EM, Peters SM. Which Clinicopathologic Factors Affect the Prognosis of Gingival Squamous Cell Carcinoma: A Population Analysis of 4,345 Cases. J Oral Maxillofac Surg. 2019 May;77(5):986-993.
2. Chen CM, Chu TH, Chou CC, Chien CY, Wang JS, Huang CC. Exosome-derived microRNAs in oral squamous cell carcinomas impact disease prognosis. Oral Oncol. 2021 Sep;120:105402.
3. Lu C, Lewis JS Jr, Dupont WD, Plummer WD Jr, Janowczyk A, Madabhushi A. An oral cavity squamous cell carcinoma quantitative histomorphometric-based image classifier of nuclear morphology can risk stratify patients for disease-specific survival. Mod Pathol. 2017 Dec;30(12):1655-1665.
4. Amarasinghe HK, Johnson NW, Lalloo R, Kumaraarachchi M, Warnakulasuriya S. Derivation and validation of a risk-factor model for detection of oral potentially malignant disorders in populations with high prevalence. Br J Cancer. 2010 Jul 27;103(3):303-9. doi: 10.1038/sj.bjc.6605778.
5. Brocklehurst P, Kujan O, O'Malley LA, Ogden G, Shepherd S, Glenny AM. Screening programmes for the early detection and prevention of oral cancer. Cochrane Database Syst Rev. 2013 Nov 19;2013(11):CD004150.
6. Manjunathan R, Jayaraman S, S R, Ileng Kumaran R, Chandrakesan P, Rajagopal P, Sambandam Y. Reactive oxygen species in oral squamous cell carcinoma progression and importance of stem cells in cancer therapeutics. In Handbook of oxidative stress in cancer: therapeutic aspects 2022 Mar 15 (1-24).
7. Sivasakthivel S, Ramani P, Poothakulath Krishnan R. Systematic Review and Meta-Analysis on Angiotensin Converting Enzyme 2 in Head and Neck Region. Cureus. 2023 Jan 11;15(1):e33673.
8. Sasahira T, Kirita T. Hallmarks of Cancer-Related Newly Prognostic Factors of Oral Squamous Cell Carcinoma. Int J Mol Sci. 2018 Aug 16;19(8):2413.
9. Thompson L. World Health Organization classification of tumours: pathology and genetics of head and neck tumours. Ear Nose Throat J. 2006 Feb;85(2):74.
10. Candé C, Cohen I, Daugas E, Ravagnan L, Larochette N, Zamzami N, Kroemer G. Apoptosis-inducing factor (AIF): a novel caspase-independent death effector released from mitochondria. Biochimie. 2002 Feb-Mar;84(2-3):215-22.
11. Sherr CJ. G1 phase progression: cycling on cue. Cell. 1994 Nov 18;79(4):551-5.
12. Ahonen TJ, Xie J, LeBaron MJ, Zhu J, Nurmi M, Alanen K, Rui H, Nevalainen MT. Inhibition of transcription factor Stat5 induces cell death of human prostate cancer cells. J Biol Chem. 2003 Jul 18;278(29):27287-92.
13. Dixon DP, Fordham-Skelton AP, Edwards R. Redox regulation of a soybean tyrosine-specific protein phosphatase. Biochemistry. 2005 May 31;44(21):7696-703.
14. Bispo de Jesus M, Zambuzzi WF, Ruela de Sousa RR, Areche C, Santos de Souza AC, Aoyama H, Schmeda-Hirschmann G, Rodríguez JA, Monteiro de Souza Brito AR, Peppelenbosch MP, den Hertog J, de Paula E, Ferreira CV. Ferruginol suppresses survival signaling pathways in androgen-independent human prostate cancer cells. Biochimie. 2008 Jun;90(6):843-54.
15. Rengarajan T, Keerthiga S, Duraikannu S, Periyannan V. Exploring the anti-cancer and anti-inflammatory activities of ferruginol in MCF-7 breast cancer cells. Cancer. 2020;1(4):1-2.
16. Jia Y, Wu C, Zhang B, Zhang Y, Li J. Ferruginol induced apoptosis on SK-Mel-28 human malignant melanoma cells mediated through P-p38 and NF-κB. Hum Exp Toxicol. 2019 Feb;38(2):227-238.
17. Pathan M, Keerthikumar S, Ang CS, Gangoda L, Quek CY, Williamson NA, Mouradov D, Sieber OM, Simpson RJ, Salim A, Bacic A, Hill AF, Stroud DA, Ryan MT, Agbinya JI, Mariadason JM, Burgess AW, Mathivanan S. FunRich: An open access standalone functional enrichment and interaction network analysis tool. Proteomics. 2015 Aug;15(15):2597-601.
18. Szklarczyk D, Santos A, von Mering C, Jensen LJ, Bork P, Kuhn M. STITCH 5: augmenting protein-chemical interaction networks with tissue and affinity data. Nucleic Acids Res. 2016 Jan 4;44(D1):D380-4.
19. Shannon P, Markiel A, Ozier O, Baliga NS, Wang JT, Ramage D, Amin N, Schwikowski B, Ideker T. Cytoscape: a software environment for integrated models of biomolecular interaction networks. Genome Res. 2003 Nov;13(11):2498-504.

20. Jejurikar BL, Rohane SH. Drug designing in discovery studio. 2021, 135-138.
21. Jayaraman S, Natararaj S, Veeraraghavan VP. Hesperidin Inhibits Oral Cancer Cell Growth via Apoptosis and Inflammatory Signaling-Mediated Mechanisms: Evidence From In Vitro and In Silico Analyses. Cureus. 2024 Feb 2;16(2):e53458.
22. Jayaraman S, Natarajan SR, Veeraraghavan VP, Jasmine S. Unveiling the anti-cancer mechanisms of calotropin: Insights into cell growth inhibition, cell cycle arrest, and metabolic regulation in human oral squamous carcinoma cells (HSC-3). J Oral Biol Craniofac Res. 2023 Nov-Dec;13(6):704-713.
23. Lee TY, Tseng YH. The Potential of Phytochemicals in Oral Cancer Prevention and Therapy: A Review of the Evidence. Biomolecules. 2020 Aug 6;10(8):1150.
24. Mascitti M, Orsini G, Tosco V, Monterubbianesi R, Balercia A, Putignano A, Procaccini M, Santarelli A. An Overview on Current Non-invasive Diagnostic Devices in Oral Oncology. Front Physiol. 2018 Oct 25;9:1510.
25. Quan H, Shan Z, Liu Z, Liu S, Yang L, Fang X, Li K, Wang B, Deng Z, Hu Y, Yao Z, Huang J, Yu J, Xia K, Tang Z, Fang L. The repertoire of tumor-infiltrating lymphocytes within the microenvironment of oral squamous cell carcinoma reveals immune dysfunction. Cancer Immunol Immunother. 2020 Mar;69(3):465-476.
26. Anand R, Dhingra C, Prasad S, Menon I. Betel nut chewing and its deleterious effects on oral cavity. J Cancer Res Ther. 2014 Jul-Sep;10(3):499-505.
27. Yang WE, Chen YT, Su CW, Chen MK, Yeh CM, Chen YL, Tsai MY, Yang SF, Lin CW. Hispolon induces apoptosis in oral squamous cell carcinoma cells through JNK/HO-1 pathway activation. J Cell Mol Med. 2023 May;27(9):1250-1260.
28. Pazhani J, Jayaraman S, Veeraraghavan VP. Therapeutic implication of chimeric antigen receptor T-cell therapy for head and neck squamous cell carcinoma. Int J Surg. 2023 Mar 1;109(3):230-231.
29. León X, Orús C, Casasayas M, Neumann E, Holgado A, Quer M. Trends in disease-specific survival of head and neck squamous cell carcinoma patients treated in a single institution over a 30-year period. Oral Oncol. 2021 Apr;115:105184.
30. Lin HL, Chen PR, Mao CC, Zheng WE, Wang JQ. Ferruginol-induced apoptosis in Human Colon Cancer Cells (HCT-116) through the mitochondria-mediated apoptotic pathway. Pharmacognosy Magazine. 2021;17(74).
31. Ho ST, Tung YT, Kuo YH, Lin CC, Wu JH. Ferruginol inhibits non-small cell lung cancer growth by inducing caspase-associated apoptosis. Integr Cancer Ther. 2015 Jan;14(1):86-97.
32. Shao L, González-Cardenete MA, Prieto-Garcia JM. In Vitro Cytotoxic Effects of Ferruginol Analogues in Sk-MEL28 Human Melanoma Cells. Int J Mol Sci. 2023 Nov 14;24(22):16322.
33. Luo G, Zhou J, Li G, Hu N, Xia X, Zhou H. Ferruginol Diterpenoid Selectively Inhibits Human Thyroid Cancer Growth by Inducing Mitochondrial Dependent Apoptosis, Endogenous Reactive Oxygen Species (ROS) Production, Mitochondrial Membrane Potential Loss and Suppression of Mitogen-Activated Protein Kinase (MAPK) and PI3K/AKT Signaling Pathways. Med Sci Monit. 2019 Apr 21;25:2935-2942.
34. Zhu XY, Zhang CL, Lin Y, Dang MY. Ferruginol alleviates inflammation in dextran sulfate sodium-induced colitis in mice through inhibiting COX-2, MMP-9 and NF-κB signaling. Asian Pacific J Tropical Biomed 2020; 10:308-315.